ISSN (Print) 1226-1750
ISSN (Online) 2233-6656
Journal of Magnetics 22(3), 430-434 (2017) https://doi.org/10.4283/JMAG.2017.22.3.430

Design Optimization of High-Speed Machines for Underwater Electric Thrusting Systems considering Magnetic Flux Density Distribution

Jung-Hyung Park[1], Kyu-Seok Lee[2], Sung-Ho Lee[2], and Sang-Yong Jung[1]*

[1]*School of Electronics and Electrical Engineering, Sungkyunkwan University, Suwon 16419, Korea*
[2]*Seonam Regional Division, Korea Institute of Industrial Technology, Gwangju 61012, Korea*

(Received 31 May 2017, Received in final form 4 August 2017, Accepted 5 September 2017)

This paper presents an optimization design and experiment of a high speed motor (HSM) for underwater thrusting systems by using magnetic flux density distribution (MFDD) of the stator, based on finite element analysis (FEA). The MFDD in the HSM is closely related to the electro-magnetic loss. This is an important factor when considering increasing efficiency, miniaturization, and reducing overall weight. To this end, a volumetric design of the rotor, which directly affects the magnetic flux density (MFD), was carried out using torque per rotor volume and a design line of electro-motive force. Calculation of the MFDD of the stator was derived from the area of the triangular element by the 2-D finite element method using the element node and the center of gravity. The flux density inside the element was derived by FEA. The maximum density distribution (MDD) and average density distribution (ADD) of the MFDD for the variable area (yoke, tooth, and shoe) of the stator core are presented. Efficiency optimization was performed by calculating the iron loss and efficiency reduction ratio using the ADD. On the basis of the manufactured 2.5 [kW] HSM, the optimal design of the MFDD was verified by comparing the FEA results with the experimental results at the rated operating point.

Keywords : optimal design, magnetic flux density distribution, iron losses, high-speed motor, underwater thrust

1. Introduction

Recently, high-speed electrical machines have been widely used in various industries because they can be made to be highly efficient, compact, and light-weight under the same power and current density conditions as the operating speed increases [1]. The development of underwater research, including fisheries, harbor surveillance systems, and military underwater robot research are being commercialized in various forms, utilizing remotely operated vehicles and autonomous underwater vehicles, depending on the field of use. With respect to underwater mobile robots, the electric motor, which primarily use a permanent magnet (PM), is the most important part for driving underwater propulsion, and as such, analysis of the loss and structure of the electric motor is required, the distribution of the magnetic field could be accurately predicted to fulfill optimal design and accurate dynamic modeling [2-3]. In particular, consideration of electromagnetic losses at the design stage is very important because it determines the efficiency of the machine. Electromagnetic losses in permanent magnet devices are largely classified into copper loss, iron loss, and rotor eddy current loss [4-6]. Because the iron loss increases with operating frequency, it significantly affects the efficiency of a high-speed motor (HSM).

For this reason, this paper describes an optimal design for a HSM applied to underwater propulsion, considering the optimization of the magnetic flux density distribution (MFDD) of the stator core. In general, the electric steel sheet used for the stator core has high permeability and small iron loss at a magnetic flux density (MFD) ranging from 0.4T to 0.6T. When the motor is designed with a high MFD, the size of the stator core is increased. Therefore, it is recommended to design the magnetic flux density between 1.2T and 1.4T. We calculated the average density distribution (ADD) of the flux for the optimal design of the stator core and improved the efficiency by reducing loss. First, the area of the triangular finite element (FE) was calculated using the finite element method (FEM) and the MFDD was derived by 2-D finite element analysis (FEA). The stator core was designed optimally

*Corresponding author: Tel: +82-31-299-4952
Fax: +82-31-299-4918, e-mail: syjung@skku.edu

by calculating the iron loss per torque ratio by the MFDD per variable region. Finally, an HSM was manufactured and the optimized design was verified by comparing the result of the FEA with the experimental results at the rated operating point.

2. Rotor Design of High Speed Motor

2.1. Configuration and Design Specification

The structure of an underwater thrusting system and 8-pole/9-slot HSM is presented in Fig. 1. The design specifications are shown in Table 1. The rated speed and power of HSM are 12,000 [r/min] and 2.5 [kW], respectively. PM and core were applied to the N48H and 35PN230.

2.2. Design Line of Rotor Volume

The rotor of the HSM is composed of a PM and rotor core. The PM is the main component affecting the MFDD of the stator. The rotor volume was designed using the torque per rotor volume (TRV) method [7]. The rated torque of the HSM is 1.989 [Nm] and TRV is 42 [kNm/m^3].

Figure 2 shows the design line of the back-electromotive force (EMF) using the TRV. The initial rotor volume considering design specifications is the blue point on the TRV curve. The EMF, due to rotor diameter and stack length, changes the rotor volume linearly. The EMF changes according to the residual MDF of the PM across the design line. The blue and green points are design points

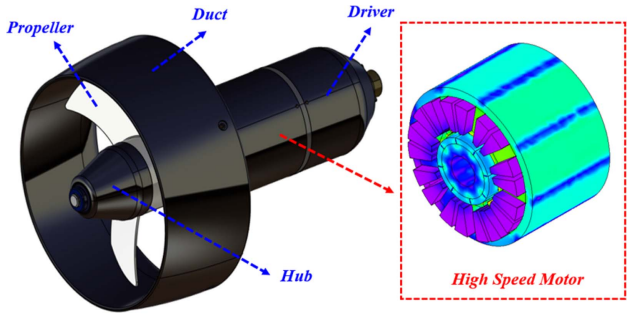

Fig. 1. (Color online) Structure of HSPM Motor. (a) Structure, (b) Magnetic flux density.

Table 1. Design specifications of high speed motor.

Parameters	Value	Parameters	Value
Number of Pole/Slot	8 Poles/9 Slots	Stator Outer Diameter	81 mm
Stack Length	50 mm	Air Gap Length	1 mm
DC Link Voltage	300 V	Phase Current	10 A

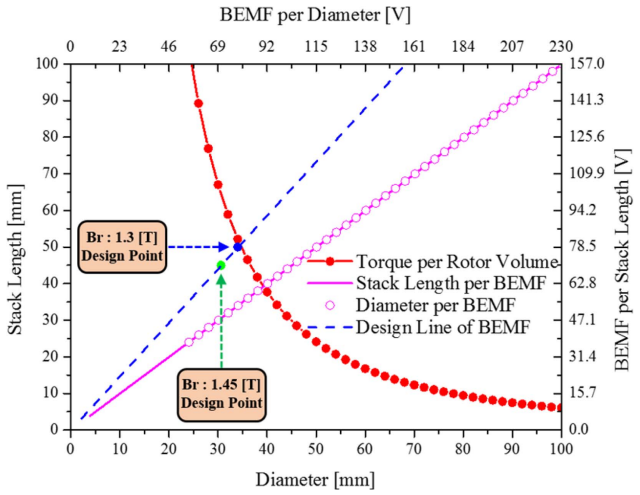

Fig. 2. (Color online) Design line of BEMF using torque per rotor volume.

with residual MFDs of 1.3 [T] and 1.45 [T] respectively. As the residual MFD of the PM increase, the volume of the rotor decreases. The residual MFD of the PM used for the optimal design is 1.4 [T]. According to the design line, the rotor diameter and stack length are 33 [mm] and 48.7 [mm]. The volume of the rotor is a fixed variables in the MFDD optimization.

3. Optimization Design of Magnetic Flux Density Distribution

3.1. Optimization Procedure

Figure 3 shows the optimal design procedure for the MFDD of the stator core.

First, the domain of the stator core is divided into the design variables yoke, tooth, and shoe. The cross-sectional area of magnetic flux linkage in each region comprises a detailed design parameter for obtaining MFDD. The optimal design of MFDD was derived by selecting detailed design

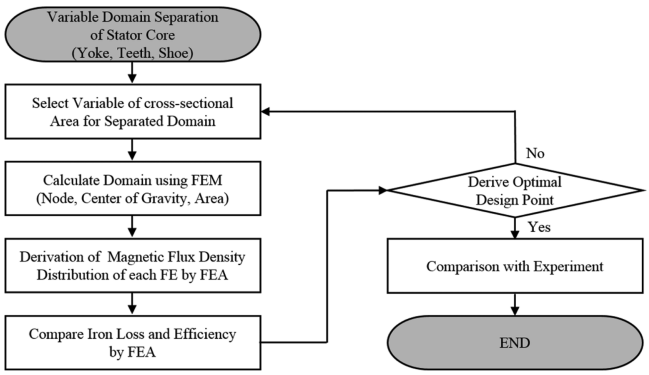

Fig. 3. Flow chart for the optimal design of magnetic flux density distribution.

parameters.

Second, the area of the triangular FE was calculated using the FEM. The MFD and iron loss were selected as the objective function and the optimal design was performed by FEA.

Third, the MFDD for the design variables was calculated by the MFD inside the FE. Based on this data, the optimal design point was derived by comparing the iron loss and efficiency of the stator core.

Finally, the optimum design of the MFDD was verified by manufacturing the HSM with the data of the optimal design point and comparing the analysis results with the experimental results.

3.2. Calculating the Area of FE

The stator core was divided into triangular FE using the FEM. The reason for calculating the area of FE is to distinguish the MFDD in the stator core in detail.

Figure 4 shows the design parameters of the stator core separated by the FEM. The nodes (Node ID, Node Position X, Node Position Y) and elements (Element ID, Position X, Position Y) of the finite element for design variables represent the vertex and center of gravity coordinates of the triangular FE. Each side of the FE is 0.2 [mm]. The number of FE varies depends on the detailed design parameters. The area of the reference element to be calculated is the vertex of the reference element with three nodes at the shortest distance from the center of gravity of the reference element in the length of all nodes.

The lengths of the three sides from the vertices of the reference element were calculated. Then, Heron's formula is applied to derive the area of the reference element. Finally, the area of the design variables represents the sum of the areas of all FEs.

3.3. Magnetic Flux Density Distribution by FEA

The FEA of the HSM was performed at the rated operating point. The MFDD for the calculated FE area is shown in Fig. 5. The MFDD when rated current flows in three phase is divided into yoke, tooth, and shoe according to the design parameters. The detailed design variables for the yoke, tooth and shoe are stator diameter, tooth width, and slot opening. The values of the detailed design parameters were chosen as 77 [mm] to 81 [mm] for the

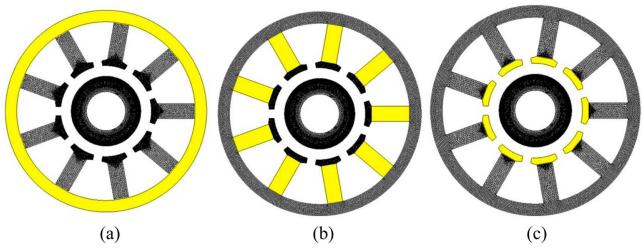

Fig. 4. (Color online) Variable domain separation of stator core. (a) yoke part, (b) tooth part, (c) shoe part.

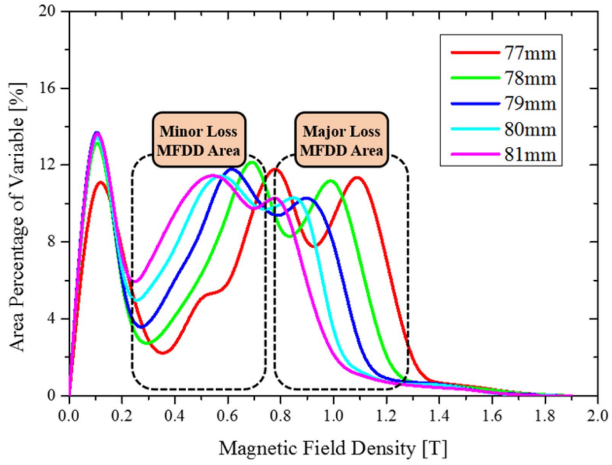

Fig. 5. (Color online) Magnetic flux density distribution by design variables. (a) yoke part, (b) tooth part, (c) shoe part.

Table 2. Magnetic flux density distribution by FEA.

Variables		MFDD		Iron Loss [W]
		MDD [T]	ADD [T]	
Yoke [mm]	77	1.231	1.10	37.432
	78	1.133	0.90	37.299
	79	1.057	0.80	34.338
	80	0.983	0.70	32.455
	81	0.948	0.75	34.189
Teeth [mm]	5.4	1.762	1.33	63.421
	5.6	1.749	1.29	56.632
	5.8	1.713	1.30	52.978
	6	1.679	1.28	49.723
	6.2	1.668	1.40	53.087
Shoe [mm]	2.8	1.735	1.25	15.653
	3	1.722	1.30	16.167
	3.2	1.704	1.25	15.611
	3.4	1.679	1.20	14.884
	3.6	1.627	1.30	15.916

outer diameter of the stator, 5.4 [mm] to 6.2 [mm] for the tooth width, and 2.8 [mm] to 3.6 [mm] for the slot opening.

The MFDD is influenced by the number of slots and the phase number of the flux linkage. The designed HSMs have a main MFDD in the 120° phase. The MFDD of the yoke is divided by half of the MFDD of the tooth, and the MFDD of the shoe is influenced by the detailed design variables. The maximum density distribution (MDD) is the maximum value of the region with the largest MFD and is generally used in machine design. On the other hand, the ADD is the average of the MFD region due to main iron loss. The ADD can be calculated as follows:

$$B_{ADD} = \frac{\sum_{n} B_{md}}{n} \quad (1)$$

where B_{md} is the MFDD calculated by multiplying the area of the unit MFD with respect to the operating frequency, and n is the number of MFDD by region of the main iron loss. The unit MFD is divided into 20 regions up to 2 [T] in 0.1 [T] units.

The results of the MFDD by the FEA are shown in Table 2. When the ADD is small, the iron loss is also small. The values of the detailed parameters of the optimal design model are yoke: 80 [mm], tooth: 6 [mm] and shoe: 3.4 [mm]. The optimal design result showed a maximum reduction in the iron loss of 19.958 [W] and an efficiency 0.914 [%] by MFD. Fig. 6 shows the iron loss density distribution of the comparative model and the optimal model.

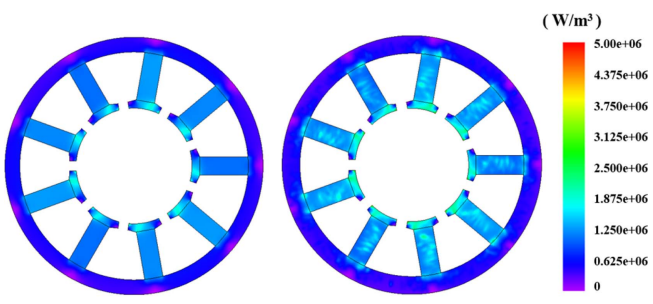

Fig. 6. (Color online) Iron loss density distribution. (a) comparative model, (b) optimal model.

4. Experimental Verification

Figure 7 and Fig. 8 shows photographs of the HSM test setting and manufactured HSM, that were employed to confirm the validity of the optimal design. The HSM was

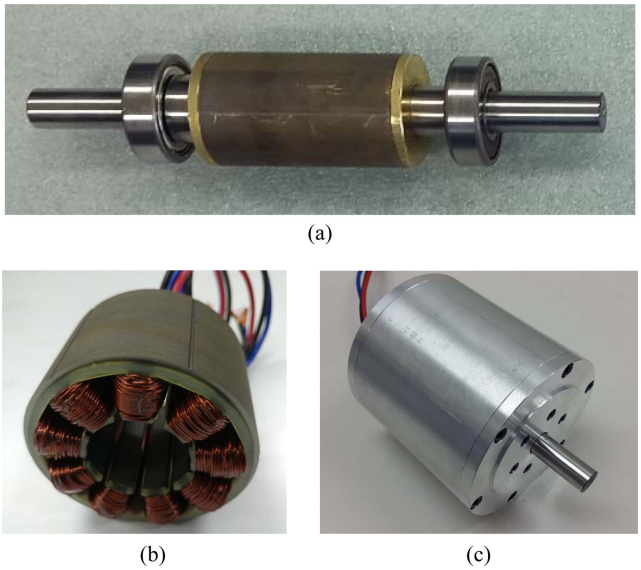

Fig. 7. (Color online) Manufactured inner rotor, stator and total assembly. (a) inner rotor, (b) stator, (c) HSM.

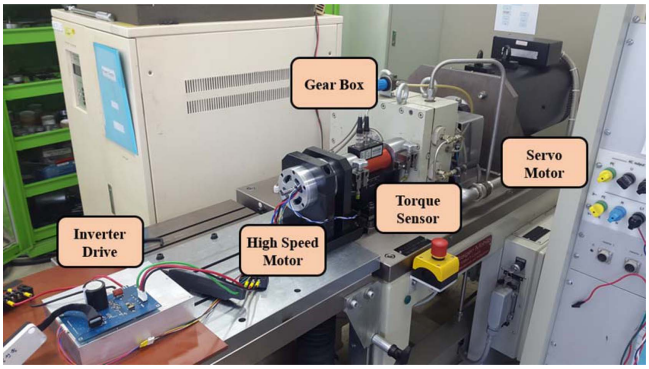

Fig. 8. (Color online) Photograph of experimental set.

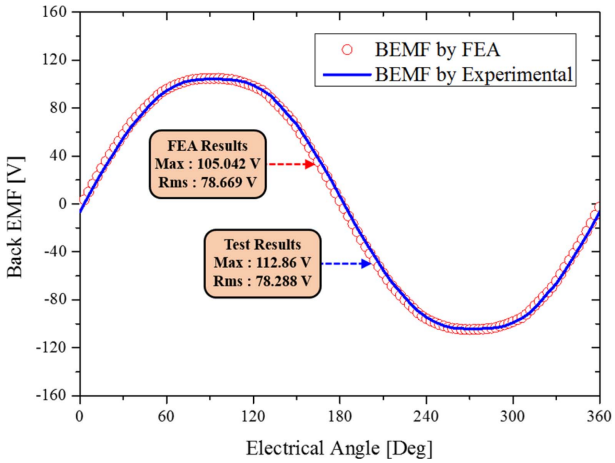

Fig. 9. (Color online) Results of BEMF by FEA and experimental.

Table 3. Comparison of HSM by rated operating point.

Parameters	Analysis Result	Measurements
Rotation Speed	12,000 rpm	12,074 rpm
Torque	2.01 Nm	1.994 Nm
Input Power	2.760 kW	2.770 kW
Output Power	2.526 kW	2.522 kW
Efficiency	91.533 %	91.055 %

driven through the inverter control and the output torque was collected through the torque sensor. The load test of the HSM was performed through the torque control of the servo motor.

Figure 9 shows the FEA and experimental results of the BEMF. The analysis result of the BEMF at 12,000 [r/min] is 78.669 [V] and the experimental results have 78.288 [V]. The BEMF error rate is 0.484 [%]. It is confirmed that the design and fabrication by the rotor volume are similar. The measured results at the rated operating point and the FEA results are summarized in Table 3. Rated torque of 1.989 [Nm] was controlled by the torque control of the servo motor. The measured torque at the rated operating point is 1.994 [Nm] which has an error rate of only 0.796 [%] as compared to the analyzed torque through FEA. In addition, the efficiency at the rated output power point differs by 0.478 [%] different. Analysis result at rated operating speed is similar to the test result.

5. Conclusion

In this study, we verified the optimal design by FEA and the experiment involving the MFDD of the HSM. First, the rotor that affects the MFDD of the stator core was designed as a fixed variable. Next, the area of the FE was calculated using FEM. Finally, the optimal design for loss reduction was performed using the ADD of the MFDD in the area of the FE. The efficiency of the HSM optimally designed with the ADD was increased by the reduction of iron loss. In addition, the optimal designed HSM was manufactured and evaluated at the actual rated operating point. The optimum design result and the measured design result were very similar.

The results of this study confirm that the optimization of the ADD of the stator core is very effective in increasing the design efficiency of the HSM and reducing the design size.

References

[1] S. M. Jang, M. M. Koo, Y. S. Park, J. Y. Choi, and S. H. Lee, IEEE Trans. Magn. **47**, 10 (2011).
[2] S. G. Kim, Y. K. Kim, G. H. Lee, and J. P. Hong, IEEE Trans. Magn. **48**, 2 (2012).
[3] J. Zou, W. Qi, Y. Xu, Y. Li, and J. Li, IEEE Trans. Magn. **48**, 11 (2012).
[4] S. M. Jang, H. W. Cho, S. H. Lee, H. S. Yang, and Y. H. Jeong, IEEE Trans. Magn. **40**, 4 (2004).
[5] K. Yamazaki, IEEE Trans. Ind. Appl. **42**, 4 (2006).
[6] K. Yamazaki, IEEE Trans. Ind. Appl. **45**, 2 (2009).
[7] J. R. Hendershot Jr, T. J. E. Miller, Design of Brushless Permanent-Magnet Machines (2010) pp. 87-92.